Mayerle, J. J., Frankel, R. B., Holm, R. H., Ibers, J. A., Phillips, W. D., & Weiher, J. F. (1973) *Proc. Natl. Acad. Sci. U.S.A. 70*, 2429–2433.
McConnell, H. M., & Chesnut, D. B. (1958) *J. Chem. Phys. 28*, 107–117.
McConnell, H. M., & Robertson, R. E. (1958) *J. Chem. Phys. 29*, 1361–1365.
Oh, B.-H., & Markley, J. L. (1990) *Biochemistry* (first paper of three in this issue).
Oh, B.-H., Mooberry, E. S., & Markley, J. L. (1990) *Biochemistry* (second paper of three in this issue).
Phillips, W. D., & Poe, M. (1973) in *Iron Sulfur Proteins* (Lovenberg, W., Ed.) Vol. II, pp 255–284, Academic Press, New York and London.
Poe, M., Phillips, W. D., Glickson, J. D., McDonald, C. C., & San Pietro, A. (1971) *Proc. Natl. Acad. Sci. U.S.A. 68*, 68–71.
Salmeen, I., & Palmer, G. (1972) *Arch. Biochem. Biophys. 150*, 767–773.
Shaka, A. J., Keeler, J., Frenkiel, T., & Freeman, R. (1983) *J. Magn. Reson. 52*, 335–338.
Skjeldal, L., Westler, W. M., & Markley, J. L. (1990) *Arch. Biochem. Biophys.* (in press).
Tsukihara, T., Fukuyama, K., Nakamura, M., Katsube, Y., Tanaka, N., Kakudo, M., Wada, K., Hase, T., & Matsubara, H. (1981) *J. Biochem. 90*, 1763–1773.
Tsukihara, T., Fukuyama, K., & Katsube, Y. (1986) in *Iron-Sulfur Protein Research* (Matsubara, H., et al., Eds.) pp 59–68, Japan Science Society Press, Tokyo.
Vold, R. L., Waugh, J. S., Klein, M. P., & Phelps, D. E. (1968) *J. Chem. Phys. 48*, 3831–3832.
Webb, G. A. (1970) *Annu. Rep. NMR Spectrosc. 3*, 211–259.
Wishnia, A. (1960) *J. Chem. Phys. 32*, 871–875.

# Nuclear Magnetic Resonance Study of Sphingomyelin Bilayers

Karol S. Bruzik,* Beata Sobon, and Grzegorz M. Salamonczyk
*Center of Molecular and Macromolecular Studies, Polish Academy of Sciences, Sienkiewicza 112, 90-362 Lodz, Poland*
*Received September 20, 1989; Revised Manuscript Received December 15, 1989*

ABSTRACT: Bilayers of D-*erythro*-(*N*-stearoylsphingosyl)-1-phosphocholine ($C_{18}$-SPM), previously characterized by differential scanning calorimetry [Bruzik, K. S., & Tsai, M.-D. (1987) *Biochemistry 26*, 5364–5368] in various phases, were studied by means of wide-line $^{31}P$, $^{2}H$, high-resolution $^{13}C$ CP–MAS, and $^{1}H$ MAS NMR. The fully relaxed gel phase of $C_{18}$-SPM at temperatures below 306 K displayed $^{31}P$ NMR spectra characteristic of the rigid phase with frozen rotation of the phosphocholine head group. Three other gel phases existing in the temperature range 306–318 K displayed spectra with incompletely averaged axially symmetric powder line shapes and were difficult to differentiate on the basis of their $^{31}P$ NMR spectra. The gel-to-gel transition at 306 K was found to be fully reversible. The main phase transition at 318 K resulted in the formation of the liquid-crystalline phase for which spectra with axially symmetric line shapes of uniform width were obtained, regardless of the nature of the starting gel phase. $^{13}C$ CP-MAS NMR spectra revealed significant differences in the molecular dynamics of sphingomyelin in various phases. All carbon atoms of the polar head group in the liquid-crystalline phase gave rise to a separate resonance lines. Numerous carbon atom signals were doubled in the stable phase, demonstrating the existence of two slowly interconverting conformers.

The calorimetric phase behavior of bilayers of fully synthetic D-*erythro*-stearoylsphingomyelin [D-*erythro*-$C_{18}$-SPM, $C_{18}$-SPM (**1**)] and of its analogues was recently studied in detail

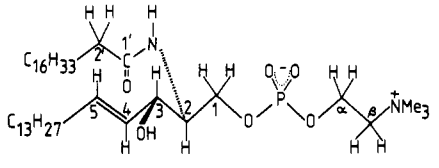

**1**

(Bruzik & Tsai, 1987; Tsai et al., 1987) and was found to be grossly different from the behavior described for racemic and semisynthetic stearoylsphingomyelin (Barenholz et al., 1976; Barenholz & Thompson, 1980; Estep et al., 1980). However, up to now, the gel and liquid-crystalline phases of pure, synthetic $C_{18}$-SPM have not been characterized by other techniques. An interesting feature of numerous sphingolipids, including currently described and non-hydroxy fatty acid cerebroside preparations, is that they can form an unusual, highly ordered stable gel phase characterized by the high enthalpy of the gel-to-liquid crystalline phase transition (Ruocco et al., 1981; Curatolo, 1987). The structure of this rigid phase remains unknown, but it has been postulated that it may play a role in biological membranes (Curatolo, 1987; Boggs, 1987). As a possible explanation of the driving force for the formation of such a rigid bilayer phase, the existence of an intermolecular hydrogen bonding network involving an amide function of the ceramide moiety has been proposed (Boggs, 1987; Lee et al., 1986).

In the currently presented work, the properties of sphingomyelin samples equivalent to those described by us earlier were studied by means of multinuclear wide-line and high-resolution NMR spectroscopy.

## Materials and Methods

$C_{18}$-SPM was synthesized and extensively purified as described recently (Bruzik, 1988a; Bruzik & Tsai, 1987). Bovine

* Address correspondence to the author.

0006-2960/90/0429-4017$02.50/0 

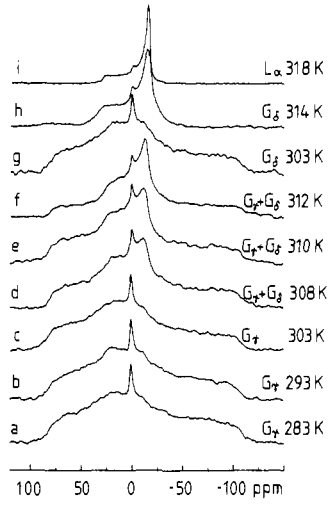


FIGURE 1: $^{31}P$ NMR spectra of dispersions of $C_{18}$-SPM. The sample was equilibrated at 283 K for 5 days, and spectra were recorded at the indicated temperatures. Spectrum g was acquired in another experiment in which the sample corresponding to trace f was quickly cooled from 312 to 303 K and the spectrum was obtained at this temperature during 1 h. Spectral parameters: sample size, 100 mg; sweep width, 62 kHz; number of transients, 3000–5000 (trace g, 1000 scans); number of data points, 512; size after FT, 4K; relaxation delay, 3 s.

brain sphingomyelin was isolated according to known procedures. The chemical purity of lipids was determined by $^{31}P$ NMR, TLC on silica gel, and differential scanning calorimetry.

The sample of $C_{18}$-SPM (150 mg) was placed in a glass ampule, water (150 mg) was added, and the sample was centrifuged through the narrow tubing in the center of the ampule at 323 K until a uniform dispersion was obtained. The sample prepared in this manner was used for $^{31}P$ NMR without opening the ampule.

All NMR spectra were obtained on a Bruker MSL-300 spectrometer using commercially available probe heads at a frequency 121.49 MHz for $^{31}P$ (10-mm broad-band probe head), 75.468 MHz for $^{13}C$, 300.13 MHz for $^{1}H$ (7-mm MAS probe head), and 46.07 MHz for $^{2}H$ (high-power probe). $^{31}P$ NMR spectra were obtained by using a Hahn echo pulse sequence (7-$\mu$s 90 deg pulse, 10-$\mu$s echo delay) with dipolar decoupling during acquisition. Typically, 512 1K data points were acquired, and the data set was zero-filled to 4K prior to Fourier transformation. Exponential multiplication with a 300-Hz (Figure 1) and a 100-Hz (Figure 2) line broadening factor was applied. Chemical shifts were externally referenced to 85% $H_3PO_4$.

For $^{13}C$ CP-MAS (cross-polarization magic-angle spinning) experiments, the 7-mm rotor was filled with the lipid dispersion, the polypropylene cap was fitted, and the rotor was sealed with cyanoacrylic glue. $^{13}C$ CP-MAS spectra were obtained by using a single-contact cross-polarization pulse sequence with a 5.5-$\mu$s 90 deg $^{1}H$ pulse, a 1-ms contact time, and a 50-ms acquisition/decoupling time. The scan repetition rate was 2–4 s. Usually, spinning rates in the range 3.5–5 kHz were applied. Due to significant dielectric loss of samples, the rotor temperature was calibrated with a nonspinning methanol sample subjected to the same pulse sequence. Longer acquisition times were also avoided to minimize heat absorption by the sample. FIDs were apodized using exponential multiplication (LB 20 Hz or Gaussian (LB 15 Hz, GB 0.3) window functions to emphasize spectral details. Chemical shifts were externally referenced to the carbonyl carbon signal of glycine (176.06 ppm).

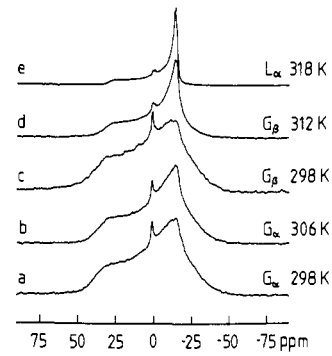


FIGURE 2: $^{31}P$ NMR spectra of bilayers of $C_{18}$-SPM with different heating/equilibration protocol: (a, b) after annealing at 320 K; (c–e) after heating above 320 K and equilibration at 293 K for 6 h. Spectral parameters: sweep width, 50 kHz; number of transients, 3000–5000; number of data points, 1K; size after transformation, 4K; relaxation delay, 1 s.

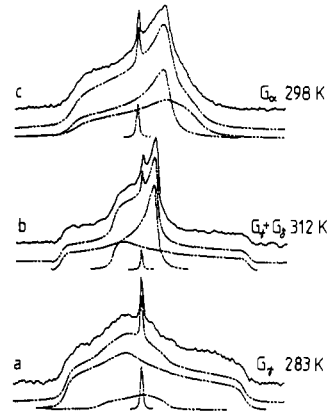


FIGURE 3: Experimental (solid line) and simulated (dashed line) $^{31}P$ NMR spectra of sphingomyelin. Experimental spectra are those from Figures 1a,f and 2a. (a) $G_\gamma$, 283 K; (b) $G_\gamma + G_\beta$, 312 K; (c) $G_\beta$ phase at 303 K. The simulated spectra are deconvoluted into three components drawn as the three bottom traces of each a, b, and c set.

## RESULTS

$^{31}P$ NMR spectra of hydrated sphingomyelin bilayers subjected to different heating/equilibration protocols are presented in Figures 1 and 2. The spectrum of the sample held at 283 K for 5 days ($G_\gamma$ phase; Bruzik & Tsai, 1987) consisted of two major lines: the broad one of a typical solid powder pattern showing three distinct chemical shielding tensors (with chemical shielding anisotropy $\sigma_{csa}$ = 184 ppm) and a small narrow peak at 0.6 ppm corresponding to an isotropic phase characterized by the rapid motional averaging of the shielding tensors. Despite our efforts to produce uniform multilamellar liposomes, the isotropic signal remained in all bilayer preparations at the level of approximately 1% of the total integrated intensity. Attempts to simulate the spectra shown in Figure 1 were made by using the iterative TENSOR simulation program (Barron, 1985). Notably, the inclusion in the simulation of the spectrum recorded at 283 K (Figure 1a) of the two above-mentioned components (static solid and isotropic) did not allow us to obtain a good fit to the experimental data. It was necessary to include in the simulation a third line (Figure 3a) with a line shape indicating almost completely averaged $\sigma_{22}$ and $\sigma_{33}$ shielding tensors. This finding reflects the contamination of the relaxed $G_\gamma$ gel phase with another gel phase ($G_\delta$) remaining at thermodynamic equilibrium at 283 K. The incomplete relaxation of the sample is ruled out based on the fact that incubation of the bilayers for longer times (up to 1 month) at 283 K had no effect on the integrated intensity of this minor component. At increasing

Table I: $^{13}C$ CP-MAS NMR Chemical Shifts (ppm) of Sphingomyelins under Different Conditions

| | $C_{18}$-SPM | | | bovine brain | | |
|---|---|---|---|---|---|---|
| function | $G_\gamma$ | $L_\alpha$ | solid anhydrous | SPM (gel) | SPM ($L_\alpha$) | $C_{18}$-SPM[g] solution |
| C-1′ | 175.1 | 175.1 | 173.75 | *a* | | 175.9 |
| | 174.0 | | | | | |
| C-5 | 134.6 | 134.3 | 132.5 | 130–135[b] | 133.9 | 135.1 |
| | 134.0 | | | | | |
| C-4 | 131.8 | 130.8 | 132.5 | 130–135[b] | 131.1 | 131.1 |
| | 129.9 | | | | | |
| C-3 | 72.9 | 71.9 | 69.1 | 72[b] | 72.0 | 72.6 |
| | 70.3 | | | | | |
| C-2 | 56.4 | 54.8 | 58.0 | *c* | 55.1 | 55.3 |
| | 52.2 | | | | | |
| C-1 | 64–68[a] | 65.9 | 63.0 | *c* | 66.1 | 65.9 |
| $C_\alpha$ | 60.8 | 60.1 | 60.7 | 60.0 | 60.0 | 60.4 |
| | 59.5 | | | | | |
| $C_\beta$ | 64–68[a] | 66.7 | 66.2 | 66.4 | *d* | 67.5 |
| NMe | 54.3 | 54.8[e] | 55.8 | 54.5 | *d* | 54.7 |
| C-2′ | | 37.1 | 37.4 | | 37.2 | 37.4 |
| $(CH_2)_n$ | 32.9 | 31.2 | 32.3 | 32.8 | 31.1 | 30.7 |
| C-3′ | 26.4 | 27.1 | 26.8 | 27.9 | 27.1 | 27.2 |
| C-17′ | 24.7 | 23.3 | 23.6 | 24.1 | 23.2 | 23.7 |
| | 24.0 | | | | | |
| Me | 14.4[f] | 14.4 | 14.5 | 14.5 | 14.2 | 14.5 |
| | | | 14.1 | | | |

[a] Several overlapped lines. [b] Broad signal centered about this value. [c] Very broad signal. [d] Signal not detected. [e] Low-intensity signal covered by signal from C-2. [f] Four closely spaced lines. [g] Data from Bruzik (1988a).

temperatures, the intensity of this slightly axially symmetric component had become more noticeable (Figures 1d–f and 3b) at the cost of the static solid powder component. The pronounced rise in the intensity of the slightly axially symmetric component occurs at temperatures close to 306 K, the temperature of the endothermic transition in the DSC curve of the studied dispersions (Bruzik & Tsai, 1987). It appears that this transition is fully reversible within the time necessary to accumulate our NMR spectra (ca. 1 h). The spectrum collected at 303 K, immediately following heating the sample at 312 K, has a very analogous appearance to the one of the equilibrated sample (traces 1c and 1g). Further heating of the sample caused the disappearance of the broad component, leaving almost exclusively the axially symmetric line shape at 314 K (spectrum 1 h), which at the temperature of the main phase transition (318 K) gave a typical line shape of a lamellar liquid-crystalline phase with more rapid averaging and the chemical shift anisotropy spanning 45 ppm. When this sample was cooled down below the main transition, the resulting metastable gel phase $G_\alpha$ at 298 K displayed only slightly axially symmetric line shape (Figure 2a). In contrast to the DSC curve, the NMR line shape was not altered by the incubation of the sample at 293 K (spectrum at 298 K, Figure 2c). Gradual heating of the dispersion in the $G_\beta$ from 298 K resulted in spectral changes characteristic of the gradual increase in the rate of the head-group reorientation (spectra 2d,e). Thus, by $^{31}P$ NMR line shape criterion, gel phases $G_\alpha$ and $G_\beta$, separated by the endotherm at 309 K, could not be distinguished. The line shapes of the spectra of both phases at lower temperatures could not be satisfactorily reproduced by simulation assuming only one axially symmetric pattern. The better fit to experimental spectra was obtained when the second component with incompletely averaged $\sigma_{22}$ and $\sigma_{33}$ was added at an approximately 1:1 ratio (Figure 3c).

$^{13}C$ CP-MAS NMR spectra of the same sample of $C_{18}$-SPM are presented in Figure 4. The spectrum of the sample in the $G_\gamma$ phase taken at 283 K displayed a doubling of all signals from the carbon atoms of the polar head group (with the exception of the choline *N*-methyl carbon). The largest splitting occurred for C-2, C-3, and C-4 carbons of the sphingosine backbone. The resonance signal from the amide

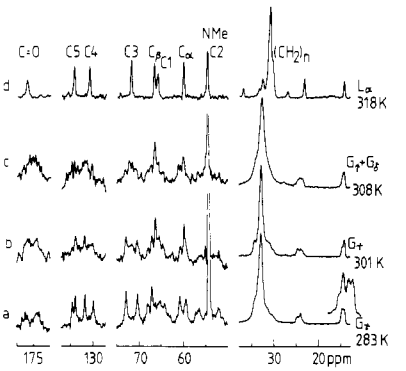


FIGURE 4: $^{13}C$ CP-MAS spectra of the dispersion of $C_{18}$-SPM. Sample conditions as in Figure 1. Spectral parameters: sweep width, 16 kHz; number of transients, 5000–7000 (except for trace d, 500 scans); number of data points, 1670; size after FT, 16K (inset in trace a was obtained with Gaussian workup, LB −10 Hz, GB 0.7 ); relaxation delay, 2 s; rotation speed, 3.3–4.0 kHz (except for trace d, 1 kHz).

carbonyl carbon was resolved into two broad signals, each of which was further split into more lines. This fact was obscured by the low signal-to-noise ratio attainable with our spectrometer. The signals from $C_\beta$ and C-1 were difficult to assign due to their multiple splitting and overlapping. The terminal methyl groups of the two hydrocarbon chains were distinguished and further split, yielding altogether four lines (see insert in trace a). The chemical shifts of the $^{13}C$ NMR signals of $C_{18}$-SPM in gel and liquid-crystalline phases are summarized in Table I. The described spectral pattern was preserved during sample heating up to 291 K (data not shown). The increase of the temperature to 301 K (Figure 4b) resulted in considerable broadening of all lines, which contributed to the rather poor signal-to-noise ratio in this case. It was possible to observe, however, another set of lines superimposing on the residual doublet pattern observed in the low-temperature spectrum. The new gel phase ($G_\delta$) displayed single signals for each carbon site, usually positioned at the exact mean value of the chemical shifts of the two lines observed in the low-temperature spectrum. At 308 K, spectral lines of the new phase predominated, and at 318 K, the lines narrowed, and all signals of the polar head group were seen separately (Figure

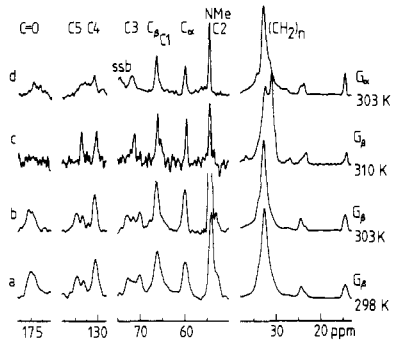


FIGURE 5: $^{13}C$ CP-MAS spectra of the dispersions of $C_{18}$-SPM in $G_\beta$ and $G_\alpha$ phases. For the $G_\beta$ phase, the sample was incubated at 293 K for 6 h. Spectral parameters: exponential multiplication of FID, 10 Hz; number of transients, 1000–1500; other parameters as in Figure 4; rotation speed, 3.5 kHz.

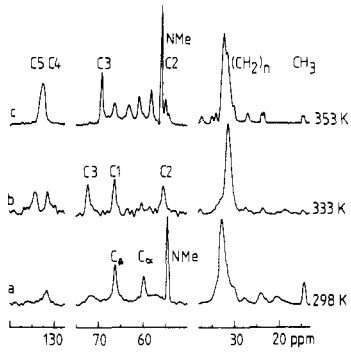


FIGURE 6: $^{13}C$ CP-MAS spectra of the dispersions of bovine brain SPM (a, b) and of anhydrous $C_{18}$-SPM (c). Spectral parameters: sample size (a, b) 40 mg, (c) 200 mg; number of transients (a, b) 1000, (c) 500. Other parameters as in Figure 4.

4d, Table I). The signal at 54.8 ppm arose most probably from C-2, or it was a composite of the low intensity signal from the choline methyl group and C-2. Analogously to the melting of the hydrocarbon chain arrays in DL-DPPC (Oldfield et al., 1987; Bruzik et al., 1989), there was an upfield shift of the methylene carbon signal upon crossing the main phase transition. It is necessary to mention here that the assignment of the lines in all $^{13}C$ MAS spectra was made on the basis only of the previous assignment of sphingomyelin (Bruzik, 1988a) and cerebroside (Sarmientos et al., 1985) spectra in solution.

The spectra of the other metastable gel phases, $G_\alpha$ and $G_\beta$, are shown in Figure 5. The metastable gel phase $G_\alpha$ yielded a $^{13}C$ CP-MAS spectrum in which signals from C-3, C-2, C-1, $C_\alpha$, and $C_\beta$ were observed (C-2, NMe, and C-1, $C_\beta$, were superimposing) and C-4, C-5, and C=O gave broad lines. The $G_\beta$ phase at 293 K exhibited doubled signals from C-3 and C-5. The other signals were similar to these in the $G_\alpha$ phase. The transition at 309 K resulted in the collapse of the signals from C-3 and C-4 to single lines (Figure 5c).

The $^{13}C$ CP MAS NMR spectra of the synthetic hydrated $C_{18}$-SPM were compared with those of solid anhydrous $C_{18}$-SPM and of hydrated bovine brain sphingomyelin. As shown in Figure 6, bovine brain SPM in its gel state at 298 K (Barenholz et al., 1976) yielded the spectrum similar to that of $C_{18}$-SPM in the $G_\alpha$ phase. In this instance, sharp lines from the choline function were detected, and lines from C-3, C-4, and C-5 were severely broadened. At 333 K, this sample existed in the liquid-crystalline state, as evidenced by the chemical shift of the signal from the hydrocarbon core (31.1 ppm). The $^{13}C$ NMR spectrum of the sphingomyelin head group in this phase consisted of relatively sharp signals from C-5 through C-1 of sphingosine, whereas the signals from the choline group were missing and the signals from the hydrocarbon terminus were observed at reduced intensities. A similar reduction in the signal receptivity was observed in the CP-MAS spectra of DL-DPPC in the liquid-crystalline phase (Bruzik et al., 1989) and of polymeric lipids at higher temperatures (Yamamobe et al., 1988). In the spectrum of solid anhydrous $C_{18}$-SPM at 353 K, most lines were displaced to such an extent that their assignment was uncertain. The lines most affected were those of C-5, C-4, C-3, and C-2 (split into two peaks). The signals from C-5 and C-4 were not resolved.

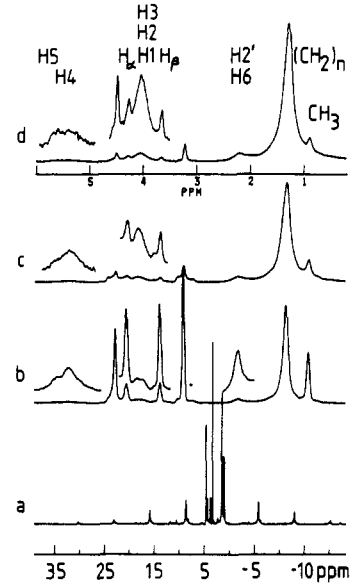


FIGURE 7: $^1H$ MAS spectra of hydrated $C_{18}$-SPM at 333 K: (a) entire spectral region showing spinning sidebands; (b) expansion of the center-band region of (a); (c, d) second and thrid spinning sideband of (a). Spectral parameters: sample size, 40 mg; sweep width, 20 kHz; 5-$\mu$s 90 deg 1H pulse; recycle delay, 1 s; number of transients, 40; Gaussian workup with LB −7 Hz, GB 0.5. Spectra were referenced with respect to the chemical shift of the hydrocarbon $CH_3$ group as $\delta$ 0.898.

$^1H$ MAS NMR spectra of sphingomyelin bilayers at 323 K (Figure 7) consisted of several lines arising from terminal methyl groups, hydrocarbon chain methylene protons, and the choline group. The remaining protons contributed broad signals at reduced intensities (e.g., stearoyl 2′-protons). This was most clearly illustrated by the large width of the resonance lines in the range 5.5–5.8 ppm (corresponding to H-4 and H-5 protons) and 4.0 ppm (from H-1, H-2, and H-3). This spectrum was clearly different from that of DPPC at 323 K (Forbes et al., 1988), whereas the signal from the glycerol H-2 at 5.3 ppm was better defined. The center band signal from methylene protons of the hydrocarbon chain was accompanied by relatively strong spinning sidebands mapping a super-Lorentzian line shape (trace a). The intensity of side bands was much lower for protons residing in a more fluid environment (choline group, hydrocarbon termini), while in the case of sphingosine H-5 to H-1 protons, relatively high intensity remained in the second and thrid sidebands (traces c and d). This reflects stronger dipolar interaction and higher $\sigma_{csa}$ for sphingosine backbone protons. The chemical shifts in the MAS spectrum correspond rather well to analogous values obtained for SPM in methanol–water solutions (Bruzik, 1988b) except for H-4 and H-5 which are shifted upfield in the bilayer state as compared to in methanol–water solution.

In order to search for hydrogen bonding in the sphingomyelin bilayers, we have measured $^2H$ NMR spectra of sphingomyelin in which the labile amide and hydroxyl protons were exchanged by deuterons. The spectra of the dispersion of $C_{18}$-SPM in $D_2O$ (Figure 8) at 320 K displayed a signal

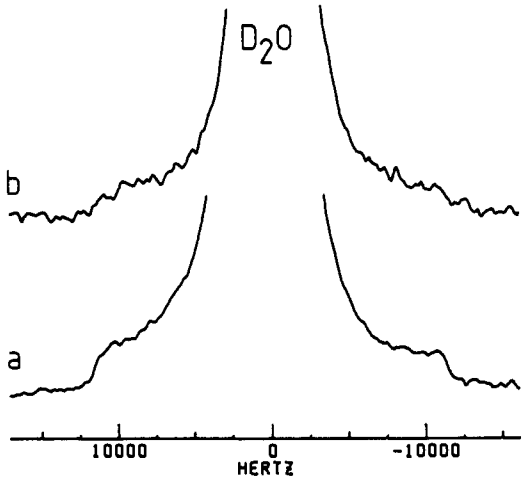


FIGURE 8: $^{2}H$ NMR spectra of dispersions of deuterated $C_{18}$-SPM at 323 K: (a) $C_{18}$-SPM in $D_2O$; (b) after adding $H_2O$. Spectral parameters: sample size, 50 mg; sweep width, 125 kHz; quadrupole echo pulse sequence; 9.5-$\mu$s 90 deg $^{2}H$ pulse; echo delay, 6 $\mu$s; number of transients, 40000; recycle delay, 0.1 s; number of data points, 512; size after FT, 4K; exponential multiplication, LB 300 Hz.

split by 22 kHz in addition to a strong central signal of deuterium oxide. The treatment of the 1:1 dispersion with a 2-fold excess of $H_2O$ (with respect to deuterium oxide) gave rise to a spectrum with only a central signal, thus indicating full exchangeability of the amide and/or hydroxyl protons with environmental water within 1 h. This experiment also sets the high limit of the exchange rate of these protons in the liquid-crystalline state of the SPM bilayer as $k_{ex} < 10^{-4}$ s$^{-1}$.

## Discussion

The results of the $^{31}P$ and $^{13}C$ NMR study of the stable $G_\gamma$ gel phase of sphingomyelin are consistent in that in this phase only very limited molecular motion is allowed. Freezing of the phosphocholine head-group rotation about a long molecular axis can originate (or may lead to) the stabilization of two conformers having, most likely, different rotation angles about C-1–C-2 and C-2–C-3 bonds of sphingosine ($\theta_1$ and $\theta_3$ angles). The conformationally induced difference in chemical shifts is largest at C-2 and amounts to 4.5 ppm. In the absence of relevant $^{13}C$ NMR data of crystalline material and of X-ray data, it is not possible to define these conformations more specifically. However, the chemical shifts of $^{13}C$ signals in the liquid-crystalline state of $C_{18}$-SPM and of bovine brain SPM (Table I) indicate that these two confomers predominate in the $L_\alpha$ phase and are approximately equally populated. The rate of the interconversion of these species in the $L_\alpha$ phase is much higher than in the $G_\gamma$ phase. The 1:1 intensity ratio of most of the doubled lines in the $G_\gamma$ phase suggests the formation of a bimolecular complex. It is possible that the amide or hydroxy proton of sphingosine and C=O functions is involved since the bilayer displays highest rigidity in the C-4–C-1 region ($^{1}H$ NMR data).

In the $G_\beta$-phase splitting of the C-3 and C-5 signals, the singlet signals of $C_\alpha$ and of C-1 and the axially symmetric line shapes of $^{31}P$ NMR spectra suggest the occurrence of the fast axial rotation of the head group about $\theta_1$ (and probably $\alpha$ angles) and restricted mobility about $\theta_3$. It is possible that the difference in $\theta_3$ between the confomers is transmitted to the phosphocholine function, and this affects the rate or tilts an axis of the phosphocholine group rotation in one conformer (with respect to the bilayer plane) resulting in the slightly different powder line shapes of the two conformers in the $^{31}P$ NMR spectrum (Figure 3c). The $G_\alpha$ phase is characterized by the faster change about $\theta_3$. The transition $G_\beta \rightarrow G_\alpha$ does not alter the head-group dynamics to an observable extent.

The remarkable suppression in the receptivity of $^{13}C$ NMR signals of the phosphocholine and hydrocarbon terminus carbon atoms in the case of bovine brain SPM and DL-DPPC as compared to analogous spectra of $C_{18}$-SPM reflects a much more fluid character of the former bilayer. $^{13}C$ NMR chemical shifts of the amorphous, anhydrous $C_{18}$-SPM indicate that the conformation in the anhydrous state of SPM is somewhat different from the one existing in the hydrated bilayers.

The current understanding of the conformationally induced $^{13}C$ shifts does not allow us to propose which conformers are involved in the equilibria in the case of highly functionalized compounds (Duddeck, 1987). To achieve this goal, further work is needed, preferably the combination of single-crystal X-ray diffraction and $^{13}C$ CP-MAS NMR.

**Registry No.** $C_{18}$-SPM, 58909-84-5.

## References

Barenholz, Y., & Thompson, T. E. (1980) *Biochim. Biophys. Acta 604*, 129–158.

Barenholz, Y., Suurkuusk, J., Mountcastle, D., Thompson, T. E., & Biltonen, R. L. (1976) *Biochemistry 15*, 2441–2447.

Barron, P. (1985) copyright Bruker (Australia) PTy., Ltd.

Boggs, J. M. (1987) *Biochim. Biophys. Acta 906*, 353–404.

Bruzik, K. S. (1988a) *J. Chem. Soc., Perkin Trans. 1*, 423–431.

Bruzik, K. S. (1988b) *Biochim. Biophys. Acta 939*, 316–326.

Bruzik, K., & Tsai, M.-D. (1987) *Biochemistry 26*, 5364–5368.

Bruzik, K. S., Salamonczyk, G. M., & Sobon, B. (1989) *Biochim. Biophys. Acta* (in press).

Curatolo, W. (1987) *Biochim. Biophys. Acta 906*, 111–136.

Duddeck, H. (1986) *Top. Stereochem. 16*, 219–324.

Estep, T. N., Calhoun, W. I., Barenholz, Y., Biltonen, R. L., Shipley, G. G., & Thompson, T. E. (1980) *Biochemistry 19*, 20–24.

Forbes, J., Husted, C., & Oldfield, E. (1988) *J. Am. Chem. Soc. 110*, 1059–1065.

Lee, D. C., Miller, I. R., & Chapman, D. (1986) *Biochim. Biophys. Acta 859*, 266–270.

Oldfield, E., Bowers, J. L., & Forbes, J. (1987) *Biochemistry 26*, 6919–6923.

Ruocco, M. J., Atkinson, D., Small, D. M., Skarjune, R. P., Oldfield, E., & Shipley, G. G. (1981) *Biochemistry 20*, 5957–5966.

Sarmientos, F., Schwarzmann, G., & Sandhoff, K. (1985) *Eur. J. Biochem. 146*, 59–64.

Tsai, M.-D., Bruzik, K. S., Wisner, D. A., & Liu, S.-L. (1987) *Biophosphates and Their Analogues—Synthesis, Structure, Metabolism and Activity* (Bruzik, K. S., & Stec, W. J., Eds.) pp 561–570, Elsevier, Amsterdam.

Yamamobe, T., Tsukahara, M., Komoto, T., Watanabe, J., Ando, I., Uematsu, I., Deguchi, K., Fujito, T., & Imanari, M. (1988) *Macromolecules 21*, 48–50.